To be submitted to
Nuclear Instr. & Meth

ISTITUTO NAZIONALE DI FISICA NUCLEARE
Laboratori Nazionali di Frascati

LNF-82/53(P)
12 Luglio 1982

P. Spillantini

HIGH BAND NEUTRINO BEAM FOR TEVATRON II

Servizio Documentazione
dei Laboratori Nazionali di Frascati

INFN - Istituto Nazionale di Fisica Nucleare
Servizio Documentazione

LNF-82/53(P)
12 Luglio 1982

HIGH BAND NEUTRINO BEAM FOR TEVATRON II

P. Spillantini
INFN - Laboratori Nazionali di Frascati, Frascati, Italy

ABSTRACT

The feasibility of a focussing system to obtain a very well collimated (quasi-ideal) parent hadron beam is discussed. It is based on the use of a specially shaped superconducting horn. For 1 TeV primary proton energy a hadron beam depleted of its low energy part (< 400 GeV) makes a spot of only 3.5 cm average radius at the end of a 500 m decay tunnel, and the separation of ν_e from ν_μ and the measurement of their energy become possible on the basis of reconstructed $K_{\mu 2}$ and K_{e3} decay kinematics. The average radius of the spot made by high energy muons ($p > 500$ GeV/c) is even smaller (2.4 cm), and a useful high energy μ-beam can be indeed obtained.

1. - INTRODUCTION

Essential features a parent hadron beam must have to allow the tagging of the energy of the neutrino coming from the K-decay are very small radius along the whole decay tunnel and poor halo around. A parent hadron beam having these features was described in (1) for the "high band neutrino beam" proposed for the SPS of CERN. It contained essentially hadrons with energy higher than half of the primary proton energy, and its spot at the end of the 400 m long decay tunnel was less than 20 cm in radius.

This work describes the feasibility of a well collimated parent hadron beam for the Tevatron II of FNAL. For a primary proton energy of 1 TeV the collection efficiency for the hadrons should be more than 50% for hadron momenta greater than 450 GeV/c, decreasing steeply to zero towards lower momenta. The focussing device mainly consists on a superconducting horn. Two observations (described in Section 2.) were applied to design the horn that would produce the higly collimated beam described in Section 3. Normally the feasibility of a new device depends on the particulars of a project. Also if I'll deal in some detail with the focusssing system, the horn

design should arouse many problems that would condition its final technical development. The horn will be limited to slow spill applications because of beam effects on the material and cooling fluids. A 10 sec spill of 10^{13}ppp gives an order of magnitude factor on the computed safety limits. The merits of the beam are discussed in Section 4. In particular a discussion is given about the possibility of using the muons from pion decay for obtaining a high energy muon beam, allowing to reduce the shielding thickness and to increase the decay tunnel length in consequence.

2. - COLLECTION OF A WIDE MOMENTUM BAND

Two observations can be made about the collection of particles from a target:

In the thin lens approximation, a single lens is able to focus a wider momentum band than any focussing-defocussing or defocussing-focussing system (see Fig. 1 and Appendix I). This implies that a horn is able to focus a wider momentum band than any quadrupole lens system.

Furthermore, if we relax the thin lens approximation, the focussed momentum band can be made even wider. In a thin lens, the focussing to infinity of particles emerging from a point source is done by a field whose strength is proportional to the distance R at which the particle enters the lens. If L(R) is the path length of the particle inside the lens and B(R) is the field strength then L(R) x B(R)=k x R in the thin lens case. Indeed, for a horn, we could contour the field and path length in different ways to approximate the thin lens case. For example:

$B(R) = k \times R$	if $L(R) =$ constant
$B(R) =$ constant	if $L(R) = L \times R$
$B(R) = k/R$	if $L(R) = L \times R^2$

In general, if $B(R) = k \times R^{\alpha}$ with $\alpha < 1$ the path of the particle in the magnetic field increases with R as $L(R) = L \times R^{(1-\alpha)}$; therefore, if $\bar{p}$ is the focussed momentum, particles with p greater than $\bar{p}$ tend to leave the field later than particles with $p = \bar{p}$ and hence undergo extra focussing. The same happens to particles with p less than $\bar{p}$, which leave the field earlier. This effect, negligible in the thin lens approximation, becomes effective as the thickness of the lens increases with respect to the focal length Z_o (see Fig. 2). In principle it should be possible to

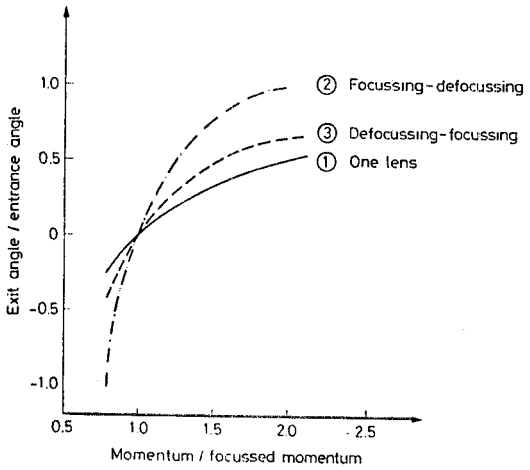

FIG. 1 - Ratio of the exit angle to the entrance angle for a particle emerging from the focus of a thin lens (curve (1)) or of a system of two thin lenses (curves (1) and (3)) as a function of the ratio of the particle momentum to the momentum fucussed at inifinity.

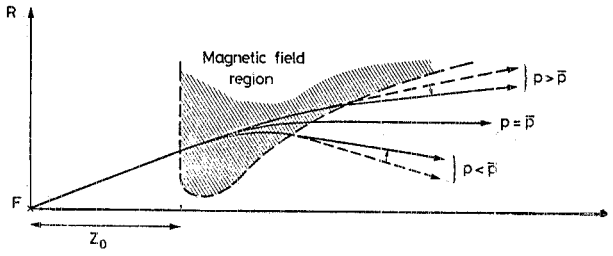

FIG. 2 - Extra-focussing effect of a thick magnetic lens due to different path lengths of a particle inside the lens: particles with p greater (smaller) than the focussed momentum $\bar{p}$ leave the field later (earlier) than particles with $p=\bar{p}$ and hence undergo a remarkable extra-focussing effect.

find a function B(R), (or possibly B(R,Z)) that will focus all momenta, but in practice the field should weaken so strongly with increasing R and/or Z that the length of the focussing system would be enormous; high momentum particles would never be able to leave the lens. However, when the ratio of the path length in the magnetic field to Z_o is as much as 10, a shape of $B(R)=k_1 R^{-1} + k_2 R^{-2}$ widens the momentum acceptance by a factor of four or five over the thin lens case. Since a field $B(R) \propto R^{-2}$ is technically difficult to achieve, a shape of $B(R) \propto R^{-1}$ is the most reasonable one to consider.

3. - A WELL COLLIMATED HIGH BAND PARENT HADRON BEAM

These concepts were applied to the problem of fabricating a parent hadron beam for Tevatron II. Choosing $Z_o=5$, and L=10 m for the length of the focusing lens, we can achieve a focussing effect as shown in Fig. 3, where the exit angle θ_{ex} is plotted as a function of the entrance angle θ_{in} for various momenta. As can be seen in this figure, particles are focussed at different $\bar{p}$ depending on θ_{in}: $\bar{p} > 600$ GeV/c for $\theta_{in}=0.2$ mrad till $\bar{p}=600$ GeV/c for $\theta_{in}=1$ mrad.

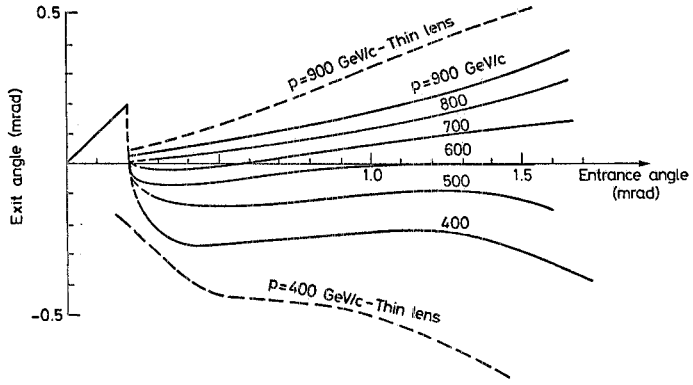

FIG. 3 - Exit angle versus entrance angle for various particle momenta. The advantage of the chosen system on the thin lens case (broken lines) is indicated for two extreme momenta.

A schematic of a section of such a lens is sketched in Fig. 4. The guiding idea is to put the s.c. wire in good thermal and electrical contact with a metallic core, which should also provide a stable mechanical support for the wire turn. The residual proton beam passes through the center without touching any element of the device.

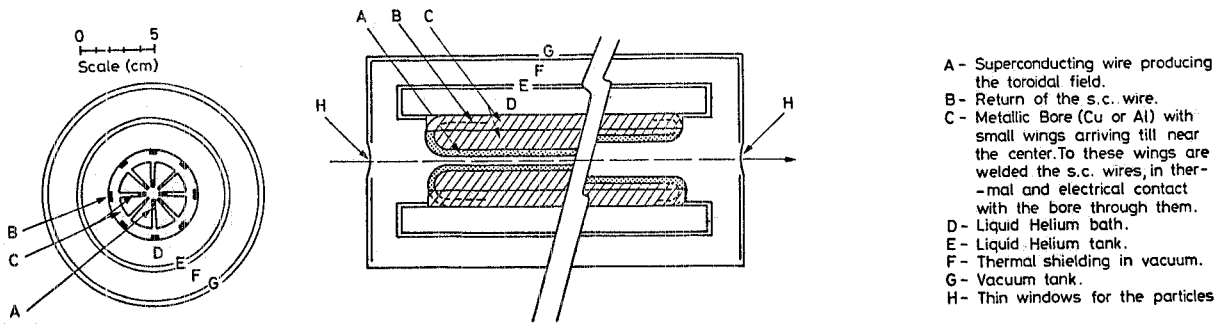

FIG. 4 - Schematic of the superconducting lens in the transversal and longitudinal sections.

The azimuthal acceptance is given in Fig. 5, from which it can be seen that some percent of the particles produced would strike the s.c. wire. Indeed an absorber, with the same shape as the metallic bore, should be placed in front of the lens to protect the s.c. wire. The absorber should not

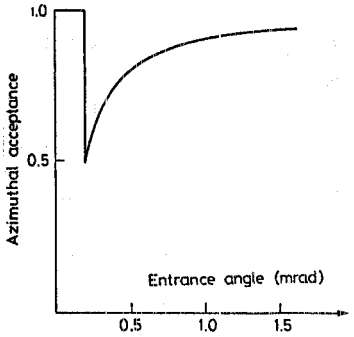

FIG. 5 - Azimuthal acceptance of the superconducting lens.

be in thermal contact with the helium bath to avoid boiling (see Fig. 6). To decrease absortion of wrong momentum and wrong sign particles in the surrounding bore with consequent high compuntion of helium, the lens

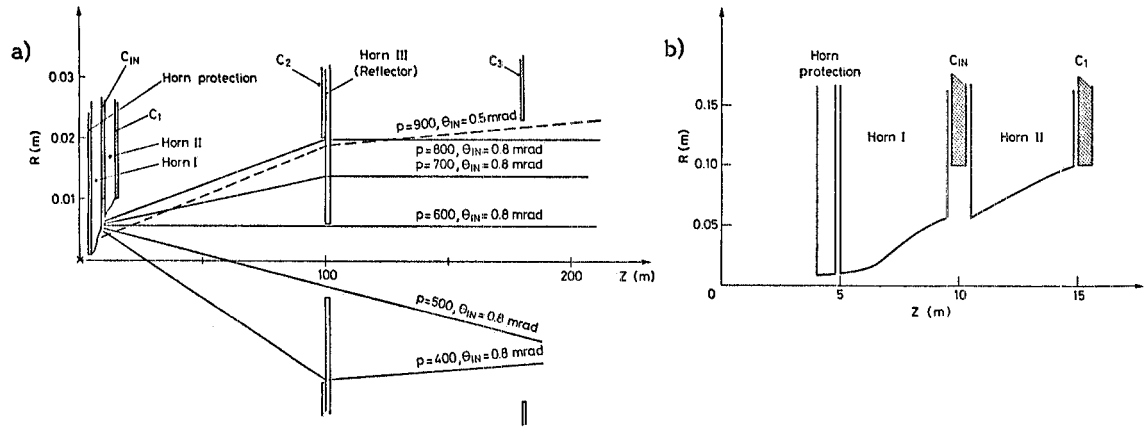

FIG. 6 - General view (a) and supeconducting magnetic horn part (b) of the collimation system used in the calculations. Typical trajectories accepted by the system are also drawn.

can be divided into sections, with absorbers interleaved between them. For the limited length of the proposed lens a division into two sections with an absorber between them (C_{IN} in Fig. 6)) would be sufficient.

The choice of the total length of the lens is a compromise: since the ratio between the path length of the particles inside the lens and the focal length Z_o is around 1, the accepted momentum band is only a factor of two greater than the thin lens case (compare in Fig. 3 the two curves for p=900 GeV/C and for 400 GeV/c); but, in this manner, the beam dimension at the exit of the lens can be mantained negligible.

The lens is supposed to carry a total current of 10kA; if the total cross section of the s.c. wires in 9 mm^2, the current density will be 1100 A/mm^2, well within the specifications of commercial s.c. wires[2]. The resulting magnetic field will be B=0.50 tesla from R=0.002 m to R=0.004 m and B(R)=0.002/R tesla for R > 0.004 m.

Two collimators (C_1 and C_2 in Fig. 6) cut the low momentum particles and define the geometry of the beam. Moreover, a third horn acting as a reflector is added downstream from the magnetic lens to improve the focussing. It profits of the fact that the lens (given the B(R) dependence of the field) focusses particles of the same momentum in a circular ring, irrespective of the entrance angle; at a suitable distance from the lens particles leaving with a different momentum pass at different distances from the axis and can be handled independtly. A bending power of (108 x R^2 – 0.039) tesla x m matches the radial distribution of the momenta at 100 m downstream from the target.

The overal view of the collimation system is given in Fig. 6. The produced parent hadron beam has a very wide momentum band (see Fig. 7) and excellent focussing properties (see Fig. 8). Throughout this study the Stefanski-White parametrization[3] was used for particle production. It was checked that the program could reproduce the neutrino flux distribution for the "perfect focussing" and "bare target" cases of the FNAL 400 GeV incident proton beam[4], as weel the "bare target" case for 1000 GeV primary proton energy reported in ref. (5).

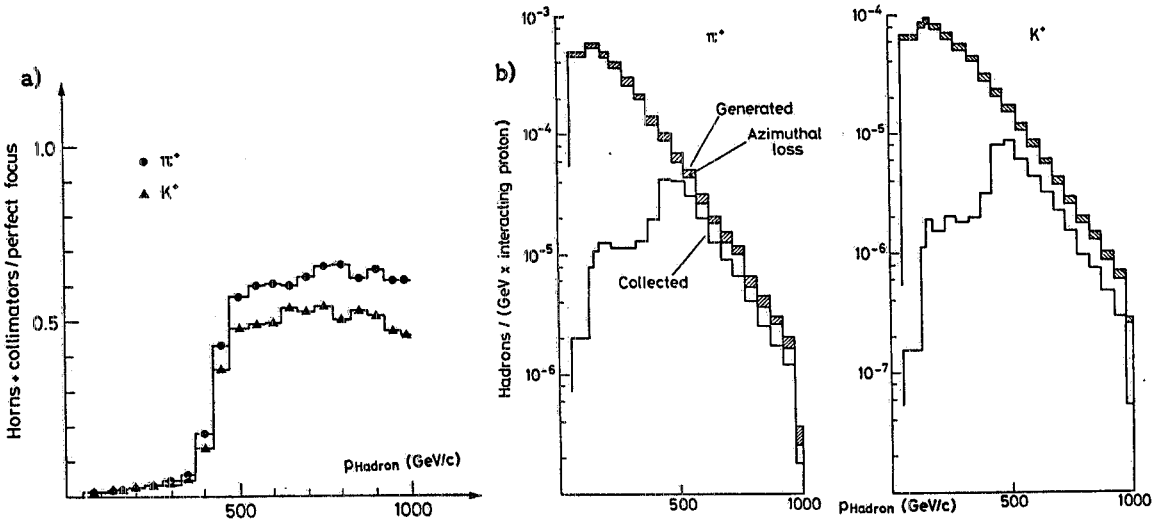

FIG. 7 - a) fraction of muons (dots) and kaons (triangles) accepted by the system as a function of their momentum. b) idem, in absolute scale.

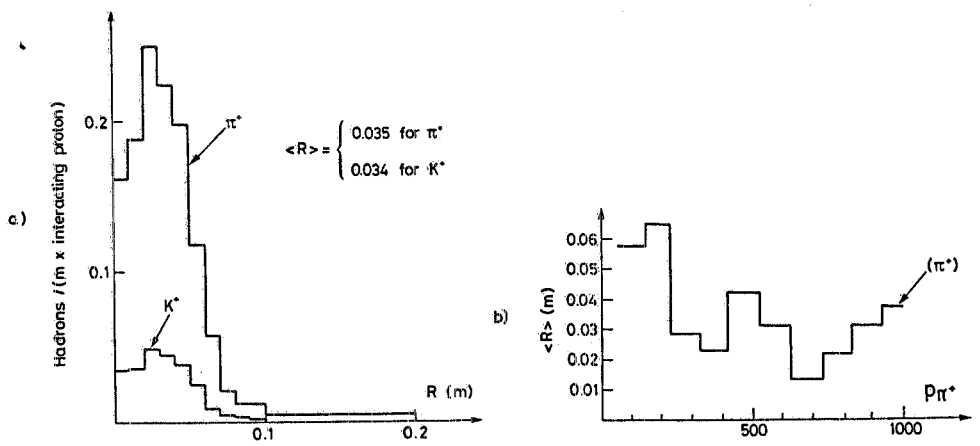

FIG. 8 - a) π^+ and K^+ radial distribution at the end of the 500 m long tunnel. b) average radius of the π^+'s at the end of the 500 m long tunnel as a function of their momentum.

The parent hadron beam produces a high band neutrino beam. Its energy spectrum at the end of a 500 m long decay tunnel is reported in Fig. 9, where it is compared with the corresponding "bare target" and "perfect focussing" spectra.

At the end of the same decay tunnel the muons have the energy spectrum of Fig. 10. Their collimation is very good, in particular for the high energy muons coming from pion decay, which give a spot of only 2.4 cm average radius (see Fig. 11).

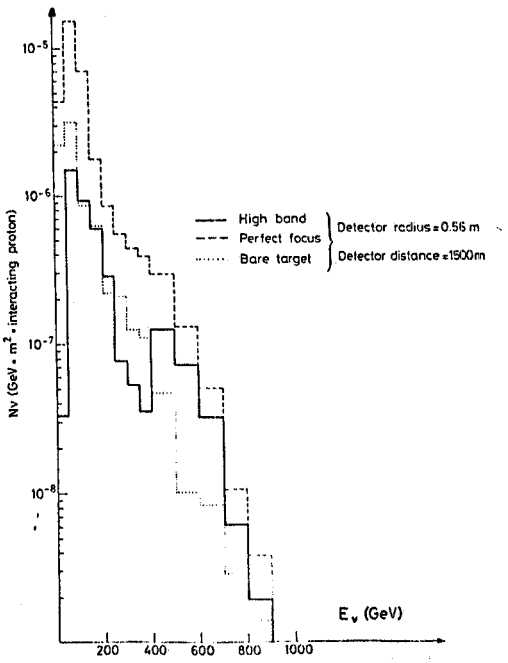

FIG. 9 - Neutrino spectrum on a surface of 1 m^2 at 1500 m down-stream from the target, compared with the bare target case (dotted line) and with the perfect focussing case (broke line).

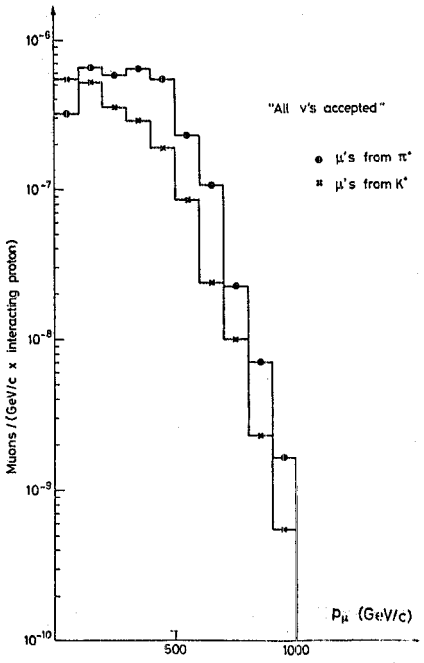

FIG. 10 - Energy spectrum of muons at the end the 500 m long decay tunnel.

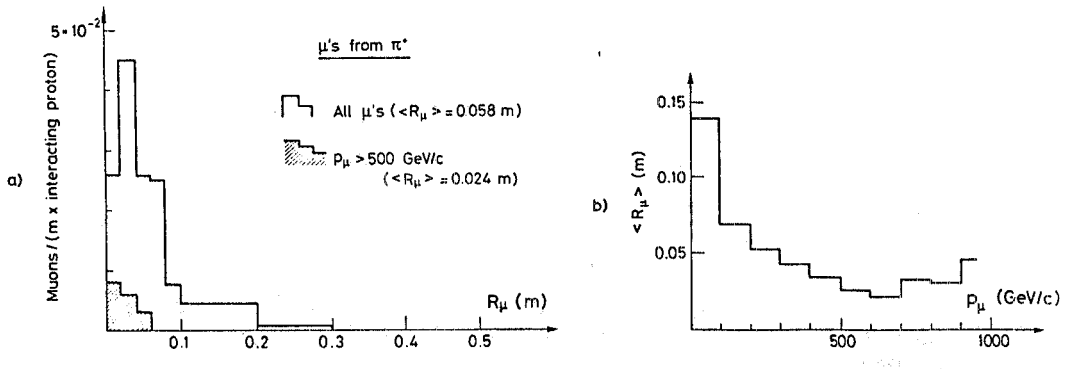

FIG. 11 - a) radial distribution of μ^+ from π^+ decay at the end of the 500 m long decay tunnel. The dashed area indicates the radial distribution of the high energy muons. b) average radius of the μ^+ from μ^+ decay as a function of their momentum.

CONCLUSIONS

Some interesting consequences of realizing a highly collimated high band parent hadron beam must be pointed out:

1) Muons from the $K \rightarrow \mu \nu_\mu$ decay have a large divergence and can therefore be detected ouside the hadron beam. This leads to the possibility of tagging the high energy part of ν_μ spectrum ($E_\nu > \frac{1}{4} E_p$).

2) The small radial dimensions of the parent beam make this tagging very clean and clear. In fact, the strong angular correlation between the event and the detected muon (see Fig. 12), together with the time coincidence gives a space matching sufficient to avoid any ambiguity in a not too sophisticade tagging system.

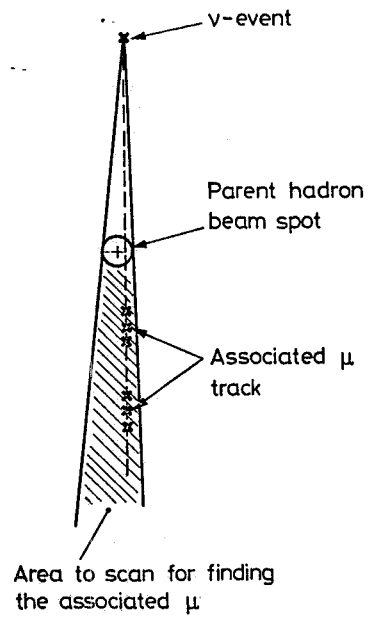

FIG. 12 - Qualitative indication of the azimuthal correlation between the ν-event position and the associated μ direction (for ν_μ from $K \rightarrow \mu \nu$ decay).

3) Also π° and electron from the $K \rightarrow \pi^\circ e \nu_e$ decay have a large divergence and therefore can be detected outside the hadron beam. This opens the actractive possibility of an efficient ν_e/ν_μ separation and ν_e energy determination.

4) The most energetic muons come from pion decay. They give a narrow spot at the end of the decay tunnel. For high energy μ's ($p > 500$ GeV/c - see Fig. 11) its average radius is only 2.4 cm. Why should we loose these muons and waste 1 km of shelding for them? Could they be bent (together with the residual proton and hadron beams) and be used for physics?

5) If the answer is yes, why not do the bending at the end of a longer tunnel (for example 1000 m long)? The total fluxes of muons and neutrinos would increase proportionally. The less energetic muons are much more open in angle and absorbed in the residual shielding. This point should be crucial for ν-beams from the future very high energy proton accelerators ($E_p \gg 1$ TeV) planned[6] or under discussion.

Finally, to illustrate the consequences 1)-3), an example of a simple tagging device is reported in Fig. 13[7]; it matches the "useful" associated μ pattern coming from the $K \rightarrow \mu$ decay (Table I).

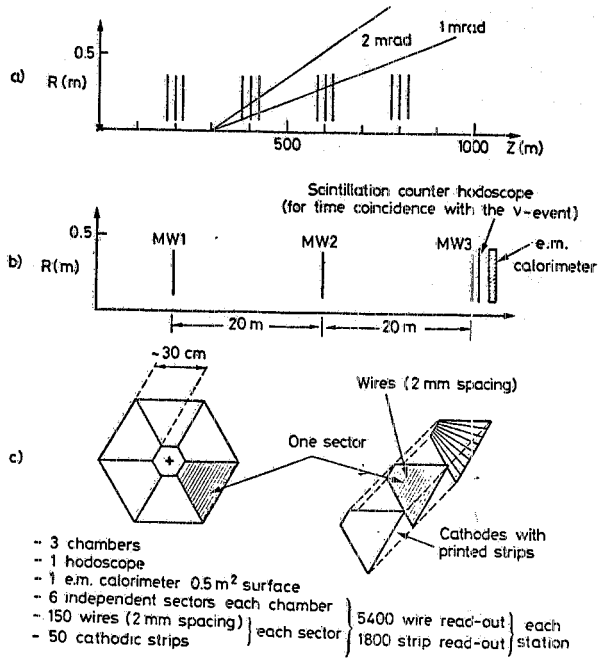

FIG. 13 - Schematic view of a simple ν_μ and ν_e tagging system composed of several measurement stations distributed along the decay tunnel (a), of a single station (b) and of a single multiwire chamber of the station (c).

TABLE I - Fraction of μ's in a $\Delta\theta_\mu \times \Delta p$ box (μ's from K – "all ν's accepted").

ΔP_μ (GeV	θ_μ (mrad)					
	0-0.2	0.2-0.4	0.4-0.6	0.6-0.8	0.8-0.1.0	1.0-2.0
0-100	0	0.001	0	0	0.003	0.238
100-200	0	0.001	0.007	0.003	0.009	0.226
200-300	0	0	0.012	0.031	0.067	0.057
300-400	0	0.007	0.040	0.092	0.013	0
400-500	0.009	0.024	0.051	0.004	0	0
500-600	0.012	0.020	0.006	0	0	0
600-700	0.005	0.004	0.001	0	0	0
700-800	0.002	0	0	0	0	0
800-900	0.001	0	0	0	0	0
900-1000	0	0	0	0	0	0
	0					
0-1000	0.030	0.060	0.116	0.131	0.092	0.568

ACKNOWLEDGMENTS

I whish to gratefully thank T.M. Taylor of CERN for his suggestions and evaluations of the proposed technical solution for the horn system, and R. Stefanski of FNAL for encouraging discussions and useful criticisms.

REFERENCES

(1) P. Spillantini, Nucl. Instr. & Meth. 123, 421 (1975).
(2) See for example the HI conductor (CU: NbTi=1.25:1, No Fil 361) furnished by the "Magnetic Corporation of America", Waltarn, Massachussetts, USA.
(3) R. Stefanski and M. White Jr., A Sign-Selected Antineutrino Beam, FNAL Report TM-626A, (1976).
(4) R. Stefanki and M. White Jr., Neutrino Flux Distributions, FNAL Report FN-292, (1976).
(5) S. Mori, "Do we need a Horn for Tevatron Neutrino Physics?", FNAL Report TM-839, (1978).
(6) L.D. Soloviev, "IHEP Accelerating storage complex", proceeding of the "1981 Inter. Symposium on Lepton and Photons Interactions at Hight Energies", Bonn, August 1981, pag. 983.
(7) In its preliminary version (P. Spillantini, FNAL report TM 1025 (1981)) the tagging device was thought to be equipped only with chambers to measure direction of charged particle. The detectors were added following a suggestion of S.P. Denisov (A.A. Voikov, S.P. Denisov, A.V. Brokhim et al. preprint IHEP 80-156, Serpukhov, 1980) for the Tagged Neutrino Facility in construction at Serpukhov.

APPENDIX

Suppose we have at a distance Z_o from a point a circular lens, able to focus at infinity all particle emerging with momentum $p=\bar{p}$ (see Fig. A1). The bending power of the lens must be proportional to the radius $\bar{R}$:

$$\frac{L(R) \times B(R)}{p} = \frac{c\bar{R}}{p}$$

(L(R) is the path length of the particle inside the lens; c is a constant)

If $L(R) \ll Z_o$ (thin lens approximation) particles with $p \neq \bar{p}$ emerge from the lens with a divergence

$$\theta_{out} = \theta_{in} - \alpha = \theta_{in} - \frac{\bar{p}}{p} = \theta_{in} \cdot \left(\frac{p-\bar{p}}{p}\right)$$

since $\alpha p = \bar{\alpha}\bar{p} = \theta_{in}\bar{p}$

The trend of the ratio $\theta_{out}/\theta_{in} = \frac{p-\bar{p}}{p}$ with $p/\bar{p}$ is given by curve 1 in Fig. 1.

If we have two thin circular lenses of opposite sign, the first at $Z_1 = Z_0$ and the second at $Z_2 = 1.5 * Z_0$, and the first one is focussing and the second one defocussing, with the notations of Fig. A2 we have:

in the I lens $\alpha_1 = \frac{\bar{\alpha}_1 \bar{p}}{p}$ with $\bar{\alpha}_1 = \frac{cR_1}{\bar{p}}$

in the II lens $\alpha_2 = \frac{\bar{\alpha}_1 \bar{p}}{p} \cdot \frac{R_2}{R_1}$

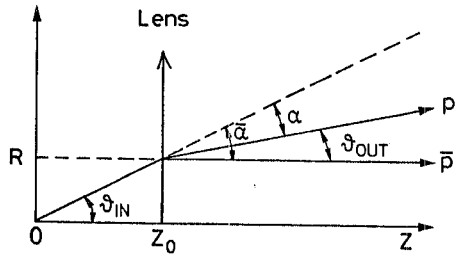

FIG. A1 - Entrance angle versus exit angle for particles crossing a thin lens placed at a Z_o distance from the particle source.

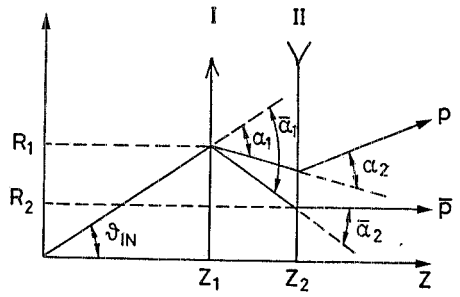

FIG. A2 - As in Fig. A1 but for a system of two lenses (focussing and defocussing) placed at $Z_1 = Z_o$ and $Z_2 = 1.5\ Z_o$ from the particle source.

For the particular geometry of Fig. A2

$$R_2 = R_1 - (Z_2 - Z_1) \cdot (\theta_{in} - \alpha_1)$$

and hence

$$\alpha_2 = \frac{\bar{\alpha}_1 \bar{p}}{p}\left(1 - \frac{Z_2 - Z_1}{R_1}(\theta_{in} - \alpha_1)\right) = \frac{\bar{1}\ \bar{p}}{p}\left(1 - \frac{1}{2\theta_{in}}(\theta_{in} - \alpha_1)\right)$$

and

$$\alpha_{tot} = \alpha_1 - \alpha_2 = \frac{\bar{1}\,\bar{p}}{p}\left(1 - 1 + \frac{1}{2}\left(1 - \frac{1}{\theta_{in}}\right)\right) = \theta_{in}\frac{\bar{p}}{p}\left(1 - 2\frac{\bar{p}}{p}\right)$$

$$\theta_{out} = \theta_{in} + \alpha_{tot} = \theta_{in}\left(1 + \frac{\bar{p}}{p}\left(1 - 2\frac{\bar{p}}{p}\right)\right)$$

The ratio θ_{out}/θ_{in} is reported as curve 2 in Fig. 1, as a function of $p/\bar{p}$. If the focussing and defocussing functions are interchanged (see Fig. A3):

$$\alpha_1 = \frac{\bar{\alpha}_1\,\bar{p}}{p} = \frac{cR_1}{p} \qquad \text{with } c = \frac{\bar{\alpha}_1\,\bar{p}}{R_1}$$

$$\alpha_2 = \frac{cR_2}{p} = \frac{\bar{\alpha}_1\,\bar{p}}{p}\,\frac{R_2}{R_1}$$

$$\frac{R_2}{R_1} = 1 + \frac{1}{2\,\theta_{in}}(\theta_{in} + \alpha)$$

$$= 1 + \frac{1}{2}(1 + \alpha_1/\theta_{in}) \ .$$

since

$$R_2 = R_1 + (Z_2 - Z_1) \times (\theta_{in} + \alpha_1)$$

hence

$$\theta_{out} = \theta_{in} + \alpha_{tot} = \theta_{in} + \alpha_1 - \alpha_2 = \theta_{in} + \frac{\bar{\alpha}_1\,\bar{p}}{p} - \frac{\bar{\alpha}_1\,\bar{p}}{p}\left(1 + \frac{1}{2}\left(1 + \frac{\alpha}{\theta_{in}}\right)\right) = \theta_{in} + \theta_{in}\frac{\bar{p}}{p}\left(-\frac{1}{2}\left(1 + \frac{\bar{p}}{p}\right)\right)$$

and the resulting ratio θ_{out}/θ_{in} is reported in Fig. 1 as curve 3.

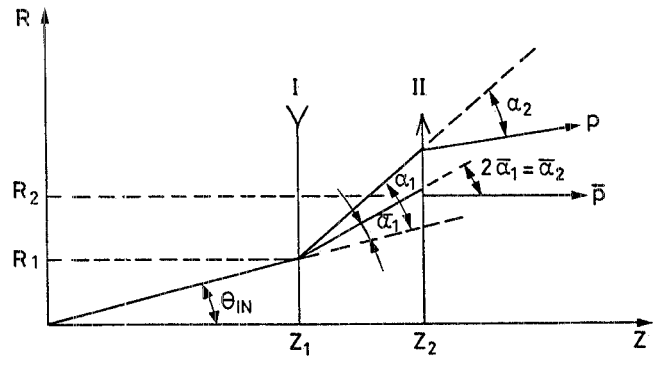

FIG. A3 - As in Fig. A1, but for a system of two lenses (defocussing and focussing) placed at $Z_1 = Z_0$ and $Z_2 = 1.5\ Z_0$ from the particle source.

Looking at Fig. 1 it appears that, for the simple geometries assumed above, the use of a lens alone allows to focus a larger band of p.

This situation is also more evident if the distance $Z_2 - Z_1$ is increased, while both the curves 2 and 3 approach the curve 1 for $Z_2 \rightarrow Z_1$ (see Fig. 1).